Case report

t(9;14)(p13;q32)/*PAX5*-IGH translocation as a secondary cytogenetic abnormality in diffuse large B-cell lymphoma

Hitoshi Ohno,[1,2)] Kayo Takeoka,[1)] Chiyuki Kishimori,[1)] Miho Nakagawa,[1)] Katsuhiro Fukutsuka,[1)]

Fumiyo Maekawa,[1)] Masahiko Hayashida,[1)] Takashi Akasaka,[2)] Shinji Sumiyoshi[3)]

A 75-year-old man presented with an ileocecal tumor composed of diffuse proliferation of large cells with immunoblastic morphology. Lymphoma cells were positive for CD20, CD79a, IRF4/MUM1, and BCL2, negative for CD5, CD10, and MYC, and partially positive for BCL6. PAX5 was positive with variable staining intensity among the cell nuclei. The V-D-J sequence of IGH showed the mutated configuration. The G-banding karyotype demonstrated two cytogenetic clones with or without t(9;14)(p13;q32), but the two shared other structural and numerical abnormalities. Fluorescence *in situ* hybridization using *PAX5* and IGH probes confirmed the presence or absence of t(9;14)(p13;q32)/*PAX5*-IGH in each clone. The breakpoints of t(9;14)(p13;q32) were mapped 2,170 bp upstream of the coding region of *PAX5* alternative exon 1B and within the IGHJ6-Eμ enhancer intron of IGH. It is suggested that t(9;14)(p13;q32) in this case was a secondary cytogenetic abnormality and the translocation is not necessarily involved in initial malignant transformation of B-cells but can occur later during the course of diffuse large B-cell lymphoma.

INTRODUCTION

Because the initial study showed that t(9;14)(p13;q32) denotes a subset of low-grade B-cell non-Hodgkin lymphoma (B-NHL) with plasmacytoid differentiation, the translocation has been described in association with lymphoplasmacytic lymphoma and other low-grade B-cell lymphomas with plasmacytic differentiation or their transformed cases.[1-3] On the other hand, t(9;14)(p13;q32) was first identified in a CD30+ diffuse large B-cell lymphoma (DLBCL) cell line, KIS-1, and we and others subsequently noted the translocation in *de novo* cases of DLBCL without preceding low-grade B-cell lymphoma.[4-7] We recently reported that patients with DLBCL carrying t(9;14)(p13;q32) presented with either nodal, extranodal, or disseminated disease and the translocation was preferentially, though not exclusively, associated with non-germinal center B-cell–like (GCB)/activated B-cell–like (ABC) phenotype of the cell of origin (COO) classification scheme.[8] As lymphoma cells uniformly expressed IRF4/MUM1, the cells are considered to exist at a late stage of B-cell differentiation between GC B-cells and terminally differentiated plasma cells, where expression of PAX5 physiologically becomes downregulated.[9] It is therefore possible that t(9;14)(p13;q32) and deregulated PAX5 expression at this particular stage of differentiation perturbs the plasma cell differentiation program initiated by PAX5 downregulation, thereby contributing to the development of DLBCL.

Here, we describe a single case of non-GCB/ABC-type DLBCL. G-banding detected t(9;14)(p13;q32) and fusion between *PAX5* and IGH was confirmed by molecular methods; however, the translocation did not represent the entire lymphoma cell population but was found in a fraction of the cells.

CASE REPORT

A 75-year-old man presented with an ileocecal tumor, which was incidentally detected on computed tomography (CT) of the abdomen for regular follow-up of biliary tract carcinoma after surgery conducted 9 years earlier. ^{18}F-fluorodeoxyglucose (FDG) positron emission tomography

(PET) combined with CT demonstrated marked uptake of the tracer in the tumor (Figure 1A). Endoscopic examination confirmed a large mass extending into the ascending colon, and biopsy disclosed DLBCL. His hemoglobin level was 10.5 g/dL, white cell count was $4.78 \times 10^3/\mu$L, and platelet count was $144 \times 10^3/\mu$L. The level of lactate dehydrogenase was 177 U/L, aspartate aminotransferase was 33 U/L, alanine aminotransferase was 19 U/L, total protein was 7.2 g/dL, albumin was 3.1 g/dL, globulin was 4.1 g/dL, creatinine was 0.8 mg/dL, uric acid was 5.5 mg/dL, C-reactive protein was 0.49 mg/dL, soluble interleukin-2 receptor was 1,192 U/mL (reference range, 145 to 519 U/mL), and β2 microglobulin was 3.67 μg/mL (reference range, 0.8 to 1.9 μg/mL). He had undergone gastrectomy for gastric cancer over 30 years previously.

Ileocecal resection was performed under open laparotomy and the surgical specimen was found to include a polypoid tumor of 6 cm in diameter that developed in the terminal ileum. After surgery, the patient received 3 cycles of R-CHOP (rituximab, cyclophosphamide, doxorubicin, vincristine, and prednisolone), followed by 3 doses of rituximab alone. He coincidentally developed carcinoma in the remnant stomach, which was treated by endoscopic submucosal dissection. He is currently free from progression of both neoplastic diseases two years after presentation.

HISTOPATHOLOGY, FLOW CYTOMETRY, AND ANTIGEN GENE REARRANGEMENT STUDIES OF SURGICAL SPECIMENS

Histopathological examination of the tumor specimens disclosed the diffuse proliferation of large cells with immunoblastic morphology (Figure 1B). The cells were positive for CD20, CD79a, IRF4/MUM1, and BCL2, and negative for CD5, CD10, and MYC, and partially positive for BCL6 by immunohistochemistry (IHC). PAX5 was positive, but the staining intensity was variable among the cell nuclei. The Ki-67 labeling index was 80 to 90% in proliferating areas (Figure 1B). Flow cytometry showed that lymphoma cells were CD5$^-$, CD10$^-$, CD19$^+$, CD20$^+$, CD21^{dim}, CD22^{dim}, CD23$^-$, CD24$^-$, CD45RA$^{-/dim}$, CD45RO^{dim}, and HLA-DR$^-$, and expressed μ and κ, and dimly expressed δ immunoglobulins on their cell surface. The DNA index was 1.00 relative to normal diploid cells.

Multiplex PCR for the antigen receptor gene rearrangements detected single species of PCR products of IGH and IGK. An IgBLAST search of the entire length of the IGH V-D-J sequence revealed that each segment matched IGHV3-7*01, IGHD6-19*01, and IGHJ3*02 sequences with 92.5% identity. The length of CDR3 in codons was 12. The tumor was negative for *MYD88*^{L265P} and *CD79B*^{Y196} mutations.

CYTOGENETIC ANALYSIS

The G-banding karyotype obtained from the tumor demonstrated two related cytogenetic clones, comprising comparable proportions among the metaphase cells analyzed; one was marked with t(9;14)(p13;q32), resulting in the characteristic 9p− and 14q+ morphology, and the other lacked the translocation. The two clones shared structural and numerical abnormalities as well as 3 unknown marker chromosomes (Figure 2A).

To confirm the presence or absence of t(9;14)(p13;q32) by fluorescence *in situ* hybridization (FISH), we applied the *PAX5* break-apart (BA) probe to metaphase spreads representing the two clones. In t(9;14)(p13;q32)-positive metaphases, der(9) at p13 and der(14) at q32 were labeled by the red-colored centromeric 5′ probe and green-colored telomeric
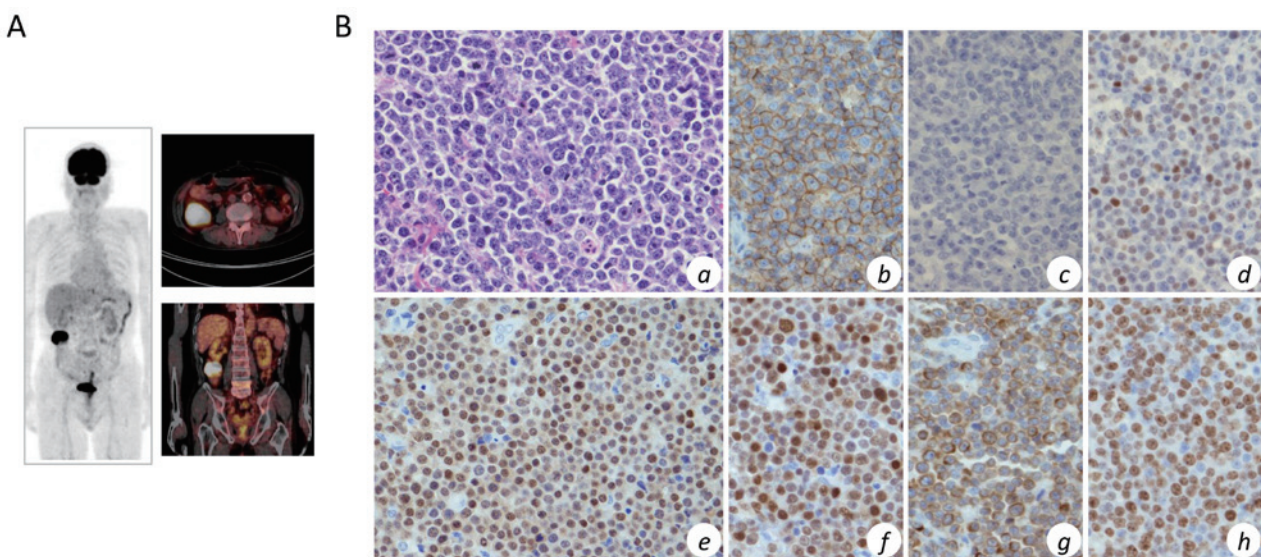

Fig. 1. (*A*) ^{18}F-FDG-PET/CT. A maximal intensity image (*left*) and combined CT and PET images (*right*) are shown. The maximum standardized uptake value of the ileocecal tumor was 29.64. (*B*) Histopathology of the ileocecal tumor. *a*, hematoxylin & eosin staining (original magnification of objective lens, ×40); *b*, anti-CD20 immunohistochemistry (×40); *c*, anti-CD10 (×40); *d*, anti-BCL6 (×40); *e*, anti-PAX5 (×40); *f*, anti-IRF4/MUM1 (×40); *g*, anti-BCL2 (×40); and *h*, anti–Ki-67 (×40).
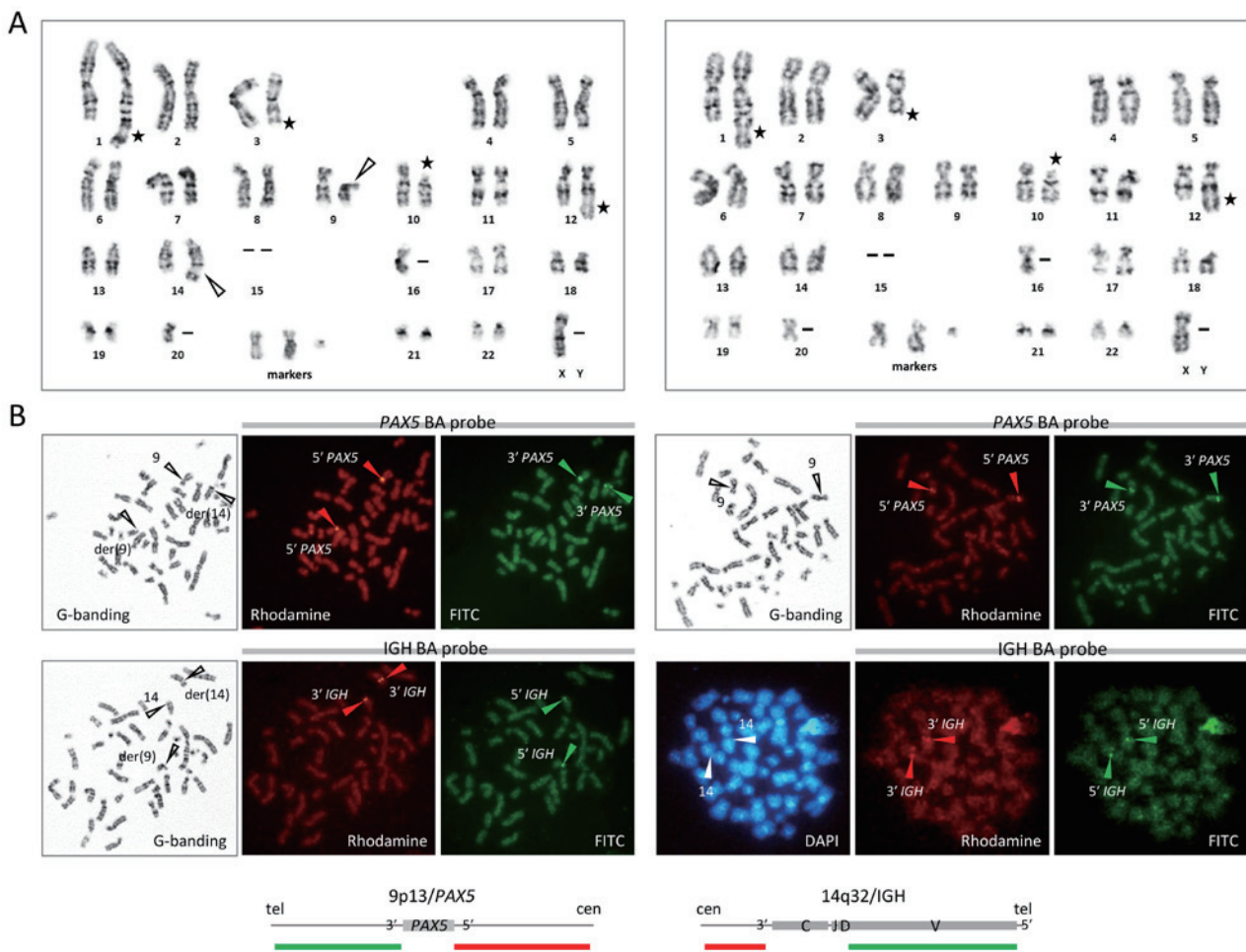
Fig. 2. Cytogenetic data. (**A**) G-banding karyotypes of t(9;14)(p13;q32)-positive (*left*) and -negative (*right*) clones. t(9;14)(p13;q32) is indicated by open arrowheads. Structural abnormalities indicated by asterisks, loss of chromosomes indicated by horizontal bars, and three marker chromosomes are shared between the two karyotypes. (**B**) FISH of t(9;14)(p13;q32)-positive (*left*) and -negative (*right*) metaphase spreads using *PAX5* (Empire Genomics, Williamsville, NY, USA) and IGH (Abbott Laboratories, Abbott Park, IL, USA) break-apart (BA) probes. Diagrams of the two probes provided by the manufacturers are shown at the *bottom*. Relevant chromosomes are indicated on G-banding or DAPI pictures and hybridization signals on rhodamine and FITC pictures are indicated by arrowheads of their respective colors. cen, centromere; tel, telomere.

3′ probe, respectively, indicating that the *PAX5* locus was disrupted between the 5′ and 3′ probes (Figure 2B, *left*). Hybridization with the IGH BA probe showed that the green-colored telomeric 5′ probe was localized at p13 of der(9) and der(14) were labeled by the red-colored centromeric 3′ probe at q32, confirming the generation of a fusion gene between 3′ *PAX5* and 3′ IGH at 14q32 and its reciprocal between 5′ IGH and 5′ *PAX5* at 9p13 (Figure 2B, *left*). In contrast, in t(9;14)(p13;q32)-negative metaphases, two homologues of chromosome 9 and those of 14 were labeled by the unrearranged *PAX5* and IGH signals, respectively (Figure 2B, *right*). No BA signals of *MYC* or *BCL6* were found in either clone (not shown). The karyotype according to the ISCN was: 44,−Y,add(1)(q42),del(3)(q25),del(10)(p11),add(12)(q24), −15,−15,−16,−20,+3mar[14]/44,idem,t(9;14)(p13;q32)[11]. ish t(9;14)(3′PAX5−,5′IGH+;3′PAX5+,5′IGH−)

ANATOMY OF THE *PAX5*-IGH JUNCTION

Two breakpoint regions of *PAX5* in t(9;14)(p13;q32) have been described; one is upstream of exon 1 and the other is immediately 5′ to the coding region of alternative exon 1B (Figure 3A).[2,3,10,11] To encompass these reported *PAX5* breakpoints, we designed oligonucleotide primers complementary to *PAX5* intron 1 (KIS-01; 5′-AAGTTGTCCTGGGCTTGGGGTC-TAAGTTTATCCTT-3′) and exon 1B (PAX5-42; 5′-TCGT-GCTTACAGTGTATTTCCATCGGGGCGCTCCA-3′) and performed DNA-based long-distance polymerase chain reaction (LD-PCR) in combination with primers for the Eμ enhancer (En) and IGHM, IGHG, and IGHA constant genes of IGH.[12,13] Approximately 3.5-kb and 6.0-kb PCR products were generated by *PAX5* exon 1B and IGH En and *PAX5* exon 1B and IGHA primer combinations (Figure 3B). Nucleotide sequencing of the former products determined that breakage and reunion occurred at 2,170 bp upstream of the coding region of *PAX5* exon 1B and 598 bp downstream of the 3′ end of the IGHJ6 segment (Figure 3C). No N-like sequences were inserted at the junction. As the result of translocation, the relevant *PAX5* and IGH sequences were fused in the divergent orientation. The generation of PCR
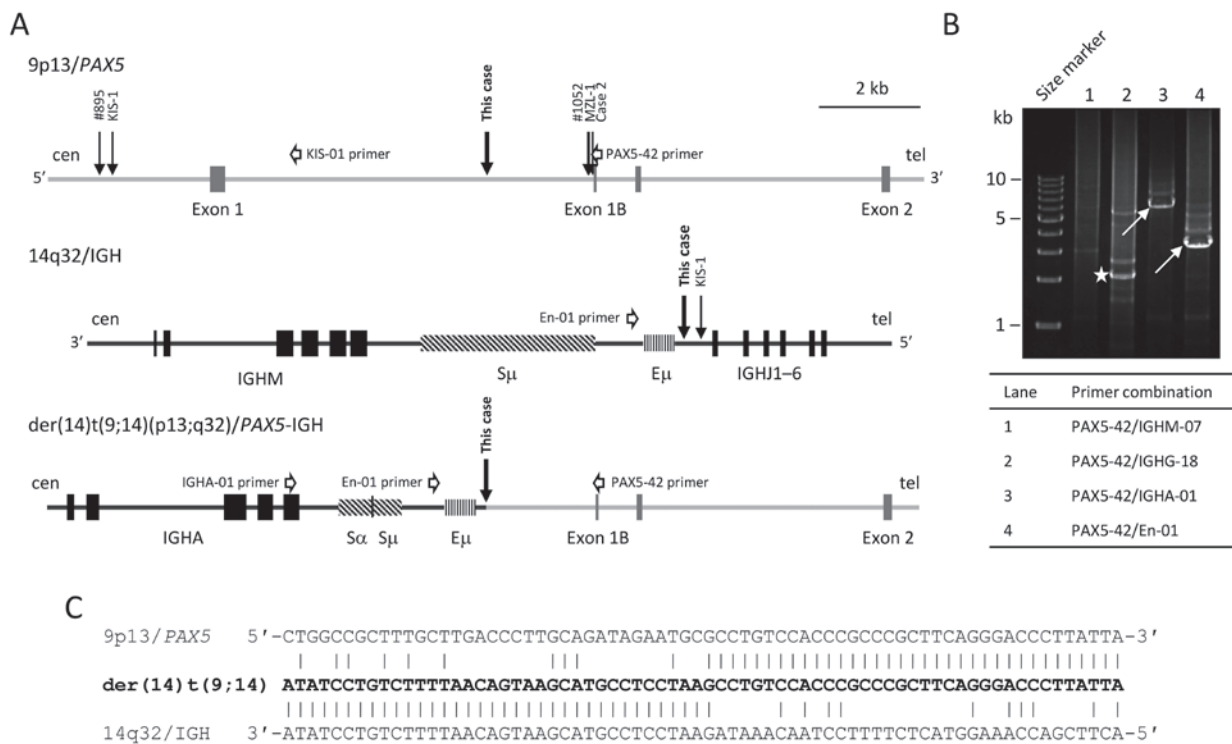
Fig. 3. Anatomy of t(9;14)(p13;q32)/*PAX5*-IGH. (*A*) Schematic diagram of the translocation. Exons 1, 2, and coding region of alternative exon 1B of *PAX5* as well as IGHJ1 to 6, Eµ enhancer, and IGHM and IGHA constant genes are presented. Sµ and Sµ/Sα switch regions are not drawn to scale. Breakpoints of reported cases and this case are indicated by vertical arrows. (*B*) Ethidium bromide-stained gel electrophoresis of LD-PCR encompassing the t(9;14)(p13;q32) junction. Arrows indicate the products amplified by PAX5-42/IGHA-01 (lane 3) and PAX5-42/En-01 (lane 4) primer combinations. PAX5-42/IGHG-18 primer combination (lane 2) generated non-specific products (asterisk). The positions of the primers are indicated in *A* and sequences of the IGH primers were described previously.[12] (*C*) Nucleotide sequences of the t(9;14)(p13;q32)/*PAX5*-IGH junction. Vertical lines indicate nucleotide identity.

products between *PAX5* exon 1B and IGHA indicated that the *PAX5*-IGH translocated allele underwent class-switch recombination from IGHM to IGHA (Figure 3A).

DISCUSSION

Here, we described a stage I DLBCL patient who presented with an ileocecal tumor. The lymphoma cells exhibited immunoblastic cell morphology with the non-GCB/ABC COO phenotype according to Hans's algorithm.[14] Accordingly, the cells carried a mutated IGH, indicating transit through GC. Most importantly, cytogenetic analysis revealed two cytogenetic clones with or without t(9;14)(p13;q32)/*PAX5*-IGH, even though the clonality of lymphoma cells was evident by the clonally rearranged IGH and IGK and expression of the single species of IGM(D)/κ immunoglobulins on their cell surface. According to the general agreement on cancer cytogenetics, t(9;14)(p13;q32) is categorized as a secondary cytogenetic abnormality in the current case.

Reciprocal chromosomal translocations between one of the three IG loci and a proto-oncogene adjacent to the breakpoint have been described in many subtypes of B-NHL.[15,16] The translocations were initially found to be selectively associated with the specific B-NHL subtype, leading to the proposal that IG translocations are the primary genetic event

involved in the development of each B-NHL subtype.[17] The most prominent examples include t(14;18)(q32;q21)/*BCL2*-IGH and t(11;14)(q13;q32)/*CCND1*-IGH, observed in 80–90% of cases of follicular lymphoma and >95% of cases of mantle cell lymphoma, respectively,[15,16] thus representing the hallmark of these two B-NHL subtypes. In contrast, t(8;14)(q24;q32)/*MYC*-IGH and the variant translocations are found in not only Burkitt lymphoma but also a significant fraction of DLBCL, and the presence of *MYC/BCL2* double-hit indicates that the *MYC*-IG translocations can secondarily occur at the time of progression from low- to high-grade lymphoma.[18] In line with this, this report suggests that t(9;14)(p13;q32) is not necessarily involved in initial malignant transformation of non-neoplastic B-cells but can occur later during the course of DLBCL. Coexistence of t(9;14)(p13;q32)-positive and -negative cells within the tumor may account for the heterogeneous staining intensity of PAX5 IHC. Nevertheless, it remains to be elucidated what effect the addition of t(9;14)(p13;q32), thereby deregulating *PAX5* expression, exerted on the tumor behavior or clinical features in this case.

Breakpoints on the proto-oncogene side in B-NHL-associated translocation are variable and occur in a large region in and around the gene, but all lead to the deregulated expression of the otherwise tightly regulated gene. In contrast, breakpoints on the IG side of translocation, in most

instances, involve either the joining (J) or switch (S) regions, suggesting that erroneous V-D-J or a class switch recombination process is responsible for the translocation.[16,19] In the current case, however, the IGH side breakpoint was 3′ to IGHJ6 and 5′ to Eμ, where either process is not operating, making the mechanism for the break unclear. Nevertheless, as a breakpoint within the IGHJ6-Eμ intron was observed in the t(9;14)(p13;q32)-carrying lymphoma cell line, KIS-1 (Figure 3A), these breakpoints may be recurrent in t(9;14) (p13;q32).[4,10] Moreover, translocated *PAX5* in both this case and KIS-1 was in close proximity to not only the Eμ intronic enhancer but also the 3′ regulatory region mapped 3′ of the IGHA constant gene.[9,19] However, this characteristic *PAX5*-IGH configuration is not always the case, as Sμ and Sα1 breakpoints have been described.[3,11] Further studies are required to determine whether the position of IGH side breakpoints reflects the primary or secondary occurrence of t(9;14)(p13;q32) during lymphomagenesis.

CONFLICT OF INTEREST

The authors declare that they have no conflict of interest.

ETHICAL APPROVAL

All procedures performed in this study involving the patient were conducted in accordance with the 1964 Helsinki declaration.

INFORMED CONSENT

The patient consented to the use of his medical records and clinical materials for research purposes.

ACKNOWLEDGMENTS

REFERENCES

1 Offit K, Parsa NZ, Filippa D, Jhanwar SC, Chaganti RS. t(9;14) (p13;q32) denotes a subset of low-grade non-Hodgkin's lymphoma with plasmacytoid differentiation. Blood. 1992; 80 : 2594-2599.

2 Iida S, Rao PH, Nallasivam P, *et al*. The t(9;14)(p13;q32) chromosomal translocation associated with lymphoplasmacytoid lymphoma involves the *PAX-5* gene. Blood. 1996; 88 : 4110-4117.

3 Morrison AM, Jäger U, Chott A, *et al*. Deregulated *PAX-5* transcription from a translocated *IgH* promoter in marginal zone lymphoma. Blood. 1998; 92 : 3865-3878.

4 Ohno H, Furukawa T, Fukuhara S, *et al*. Molecular analysis of a chromosomal translocation, t(9;14)(p13;q32), in a diffuse large-cell lymphoma cell line expressing the Ki-1 antigen. Proc Natl Acad Sci USA. 1990; 87 : 628-632.

5 Poppe B, De Paepe P, Michaux L, *et al*. *PAX5/IGH* rearrangement is a recurrent finding in a subset of aggressive B-NHL with complex chromosomal rearrangements. Genes Chromosomes Cancer. 2005; 44 : 218-223.

6 Andrieux J, Fert-Ferrer S, Copin MC, *et al*. Three new cases of non-Hodgkin lymphoma with t(9;14)(p13;q32). Cancer Genet Cytogenet. 2003; 145 : 65-69.

7 Ohno H, Nishikori M, Haga H, Isoda K. Epstein–Barr virus-positive diffuse large B-cell lymphoma carrying a t(9;14) (p13;q32) translocation. Int J Hematol. 2009; 89 : 704-708.

8 Ohno H, Nakagawa M, Kishimori C, *et al*. Diffuse large B-cell lymphoma carrying t(9;14)(p13;q32)/ *PAX5*-immunoglobulin heavy chain gene is characterized by nuclear positivity of MUM1 and PAX5 by immunohistochemistry. Hematol Oncol. 2020; 38 : 171-180.

9 Cobaleda C, Schebesta A, Delogu A, Busslinger M. Pax5: the guardian of B cell identity and function. Nat Immunol. 2007; 8 : 463-470.

10 Hamada T, Yonetani N, Ueda C, *et al*. Expression of the *PAX5 / BSAP* transcription factor in haematological tumour cells and further molecular characterization of the t(9;14)(p13;q32) translocation in B-cell non-Hodgkin's lymphoma. Br J Haematol. 1998; 102 : 691-700.

11 Sonoki T, Willis TG, Oscier DG, *et al*. Rapid amplification of immunoglobulin heavy chain switch (IGHS) translocation breakpoints using long-distance inverse PCR. Leukemia. 2004; 18 : 2026-2031.

12 Akasaka T, Kishimori C, Maekawa F, *et al*. Pulmonary extranodal marginal zone lymphoma that presented with macroglobulinemia and marked plasmacytic cell proliferation carrying the t(14;18)(q32;q21)/*MALT1*-immunoglobulin heavy-chain fusion gene in pleural fluid. J Clin Exp Hematop. 2018; 58 : 141-147.

13 Akasaka T, Akasaka H, Ohno H. Polymerase chain reaction amplification of long DNA targets: application to analysis of chromosomal translocations in human B-cell tumors (review). Int J Oncol. 1998; 12 : 113-121.

14 Hans CP, Weisenburger DD, Greiner TC, *et al*. Confirmation of the molecular classification of diffuse large B-cell lymphoma by immunohistochemistry using a tissue microarray. Blood. 2004; 103 : 275-282.

15 Willis TG, Dyer MJS. The role of immunoglobulin translocations in the pathogenesis of B-cell malignancies. Blood. 2000; 96 : 808-822.

16 Küppers R. Mechanisms of B-cell lymphoma pathogenesis. Nat Rev Cancer. 2005; 5 : 251-262.

17 Fukuhara S, Uchino H. Subclasses of 14q+ marker-positive lymphoid cancer. N Engl J Med. 1983; 308 : 1603-1604.

18 Aukema SM, Siebert R, Schuuring E, *et al*. Double-hit B-cell lymphomas. Blood. 2011; 117 : 2319-2331.

19 Burmeister T, Molkentin M, Schwartz S, *et al*. Erroneous class switching and false VDJ recombination: molecular dissection of t(8;14)/*MYC-IGH* translocations in Burkitt-type lymphoblastic leukemia/B-cell lymphoma. Mol Oncol. 2013; 7 : 850-858.